Finite Element Analysis of Tunnels in Anisotropic Rock Medium

by

K.G. Sharma*

M.K. Sharma**

Introduction

India is rich in hydro-power. There are various multipurpose river valley projects which are at different stages of planning, design, construction and instrumentation. Tunnels constitute one of the important components of these projects. For design of tunnels, the knowledge of displacements and stresses around the tunnel openings is very much required. Closed form solutions are available for regular geometric shapes such as circular, elliptical and rectangular ; and for idealized condition of geological media, viz. homogeneous, isotropic and linear elastic. However, in practice tunnels seldom have such regular shapes. Further, the geological media may be anisotropic or may have discontinuities. Such problems are not amenable to closed form solutions and one has to resort to numerical methods such as finite element method (FEM) and boundary element method (BEM). In case of non-homogeneities and anisotropy in the geological media, BEM cannot be used and FEM provides a suitable alternative. But FEM requires preparation of large input data. This difficulty can be mitigated by developing automatic data generation subroutines.

In the present paper, the finite element method has been used to analyse circular and D-type tunnels in isotropic and transversely isotropic rock mass for different insitu state of stress conditions. Plane strain case has been considered. Deformed shapes and principal stress contours have been plotted.

Anisotropy of Rock Mass

Anisotropy of rock mass is of two types—anisotropy of rock moduli and anisotropy of strength. When linear elastic model is adopted, the first type of anisotropy is considered and the second type is not relevant. When elasto-plastic analysis is carried out, then strength anisotropy is considered. In the present analysis the first type of anisotopy has been considered and the term anisotropy will refer to this type only throughout the text.

Anisotropy of rock mass is relatively less explored area inspite of the fact that anisotropy is not an uncommon phenomenon. Barla (1974) has discussed theoretical background for anisotropic analysis. Obert and

* Assistant Professor } Department of Civil Engineering, Indian Institute
** Formerly M. Tech Student } of Technology New Delhi-110016, India

Duvall (1967), and Lama and Vutukuri (1978) have presented properties of anisotropic rock masses.

In the present work, transversely isotropic rock medium has been considered. Five independent elastic constants are required to completely describe the material behaviour (Zienkiewicz, 1977). The general stress-strain relations, taking plane of stratification parallel to x-z plane and y-axis perpendicular to the plane of stratification (Fig. 1a) are given by :

$$\epsilon_x = \sigma_x/E_1 - \nu_2\,\sigma_y/E_2 - \nu_1\,\sigma_z/E_1$$

$$\epsilon_y = -\,\nu_2\,\sigma_x/E_2 + \sigma_y/E_2 - \nu_2\sigma_z/E_2$$

$$\epsilon_z = -\nu_1\,\sigma_x/E_1 - \nu_2\,\sigma_y/E_2 + \sigma_z/E_1$$

$$\gamma_{xz} = 2\,(1+\nu_1)\,\tau_{xz}/E_1 \qquad\qquad .. \;(1)$$

$$\gamma_{xy} = \tau_{xy}/G_2$$

$$\gamma_{yz} = \tau_{yz}/G_2$$

in which ϵ_x, ϵ_y, ϵ_z, γ_{xy}, γ_{yz}, γ_{xz} are strain components; σ_x, σ_y, σ_z, τ_{xy}, τ_{yz}, τ_{xz} are stress components; the constants E_1, ν_1 are associated with the behaviour in the plane of strata; and G_2, E_2, ν_2 with a direction normal to these.

After solving for stresses, Eq. (1) can be written in the matrix form as

$$\{\sigma\} = [D]\,\{\epsilon\} \qquad\qquad ...(2)$$

in which $\{\sigma\}$ is the stress vector, $\{\epsilon\}$ is the strain vector and $[D]$ is the stress-strain matrix.
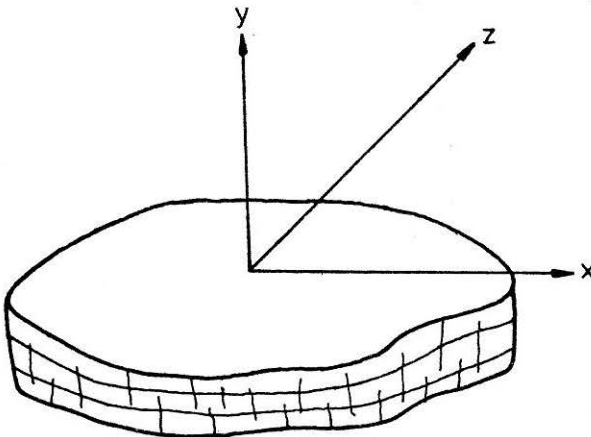
Plane of strata parallel to x - z

FIGURE 1 (a) **Transversely Isotropic Material**

For plane strain condition, $[D]$ is derived as (Zienkiewicz, 1977),

$$D = \alpha \begin{bmatrix} n(1-n\,v_2^2) & nv_2(1+v_1) & 0 \\ nv_2(1+v_1) & (1-v_1^2) & 0 \\ 0 & 0 & m(1+v_1)(1-v_1-2n\,v_2^2) \end{bmatrix} \qquad \ldots(3)$$

where

$$\alpha = \frac{E_2}{(1+v_1)(1-v_1-2n\,v_2^2)},$$

$$m = G_2/E_2 \text{ and } n = E_1/E_2.$$

The orientation of stratification in general may not coincide with x-z plane with global axes, but may be inclined at an angle β as shown in Fig. 1b. In such a case, the $[D]$ matrix given in Eq. (3) must be transformed to obtain a matrix corresponding to the global system of co-ordinates which is given by :

$$[D] = [T]^T [D'] [T] \qquad \ldots(4)$$

where $[D']$ relates the stresses and strains in the inclined co-ordinate system and $[T]$ represents a transformation matrix given by

$$[T] = \begin{bmatrix} \cos^2\beta & \sin^2\beta & -2\sin\beta \times \cos\beta \\ \sin^2\beta & \cos^2\beta & 2\sin\beta \times \cos\beta \\ \sin\beta\cos\beta & -\sin\beta\cos\beta & \cos^2\beta-\sin^2\beta \end{bmatrix} \qquad \ldots(5)$$

In Eq. (2), matrix $[D]$ is as given by Eq. (4).

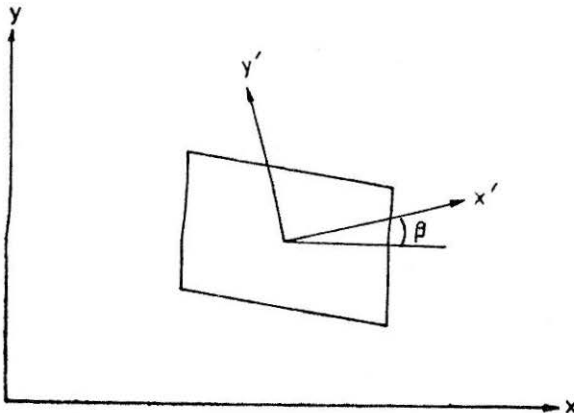

FIGURE 1 (*b*) Orientation of Stratification

With $E_1 = E_2 = E$, $\nu_1 = \nu_2 = \nu$ and $G_2 = E/2 (1+\nu)$, isotropic rock mass is represented by Eq. (3). In the present work, both isotropic and transversely isotropic rock masses have been considered.

Finite Element Method

Eight-noded isoparametric elements have been used in the present study. At each node there are two unknowns viz. horizontal displacement (u) and vertical displacement (v). Gauss Legendre numerical integration with two-sampling points has been adopted. For details on finite element formulation, refer to Zienkiewicz (1977).

The Problem

In the present study, two typical shapes viz. circular (8 m diameter) and D-type (8 m width and 8 m high) have been analysed. The overburden pressure is taken corresponding to a depth of 350 m. Three insitu stress ratios ($K_o = 0.5, 1.0, 1.5$) have been selected for this study.

Material Properties

Sharma (1984) has considered two transversely isotropic materials—Graywacke schist and Phylladesde Revin for which the properties are given in Lama and Vutukuri (1978). In the present paper, the second material is used with the following properties :

$$E_1 = 2000 \text{ MN/m}^2 \qquad E_2 = 8000 \text{ MN/m}^2$$

$$\nu_1 = 0.32 \qquad \nu_2 = 0.08$$

$$G_2 = 1240 \text{ MN/m}^2$$

The unit weight of the material is $\gamma = 0.025$ MN/m^3. Two angles of stratification (β) viz. 0° and 90° have been considered in the analysis.

Isotropic case has also been considered with the properties:

$$E = 2000 \text{ MN/m}^2 \qquad \nu = 0.3$$

$$\gamma = 0.025 \text{ MN/m}^3.$$

Analysis

Due to symmetry, quarter circular tunnel and half D-type tunnel sections have been discretized into 39 and 102 elements respectively, as shown in Figs. 2 and 3. Boundary has been taken at a distance of 4 times the diameter or width i.e. 32 m from the centre of the tunnel section. The excavation of the tunnel is considered in single stage. Induced displacements at each node and principal stresses at each Gaussian point have been computed using the computer program developed on ICL 2960 at IIT, Delhi. The nodal connectivity and nodal co-ordinates are generated by the program.
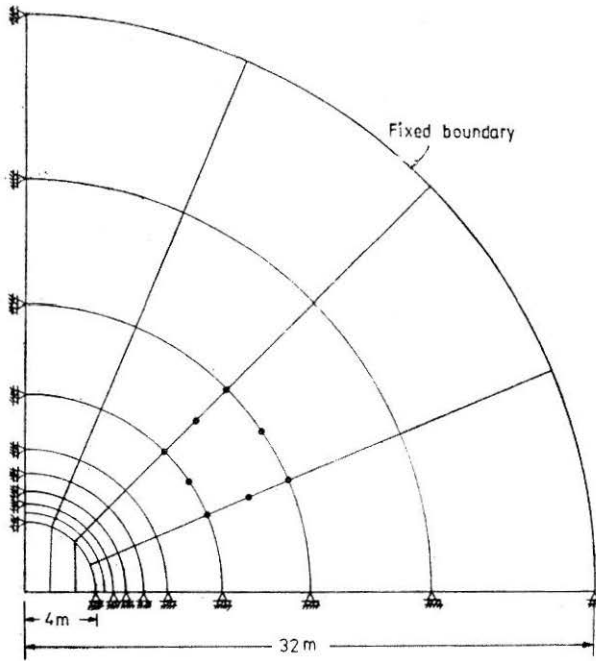
FIGURE 2 Finite Element Mesh for Circular Tunnel

Results and Discussion

Results have been presented in the form of deformed shape and principal stress contours for the various cases analysed.

Circular tunnel

(a) *Deformed Shape* : Figures 4 to 6 show the deformed shape of the circular tunnel for three insitu stress ratios (K_o) of 0.5, 1.0 and 1.5 respectively. Displacements corresponding to both isotropic and aniso-tropic cases are plotted in these figures. It is seen from these figures that the displacement at crown decreases with increase in stress ratio and reverse is the trend at the springing. The displacements are smaller for the anisotropic case as compared to isotropic case for all the three stress ratios. For $K_o = 0.5$, the deformation at the springing is negative for $\beta = 90°$ case whereas for other K_o values no negative deformation is observed at springing or at crown. It is further observed that $\beta = 0°$ gives less deformation at crown and larger displacement at springing as compared to $\beta = 90°$. Thus anisotropy has marked effect on the deformed shape of the circular tunnel.

(b) *Principal Stresses*: The principal stresses have been plotted in the form of contours. Figures 7 to 9 show the major and minor principal stress contours for three stress ratios respectively. In each figure, the contours corresponding to the three cases (isotropic, anisotropic with $\beta = 0°$ and 90°) have been plotted together to facilitate comparison. As is seen from Fig. 7 for $K_o = 0.5$, the contours for isotropic and $\beta = 90°$ cases
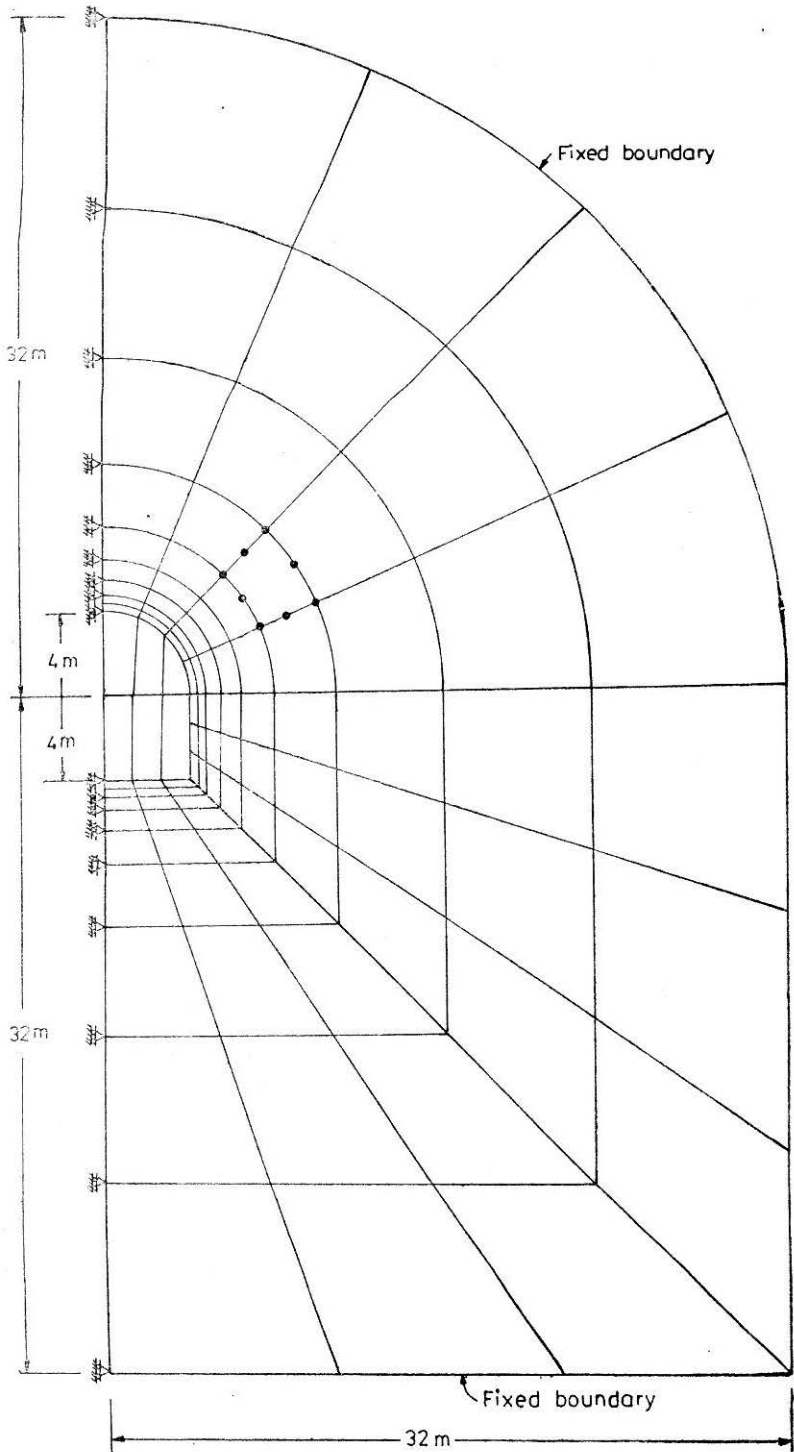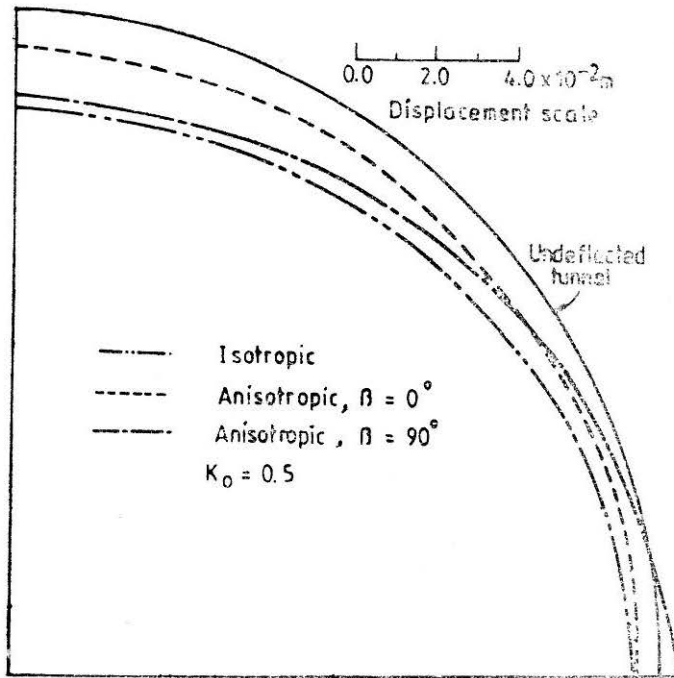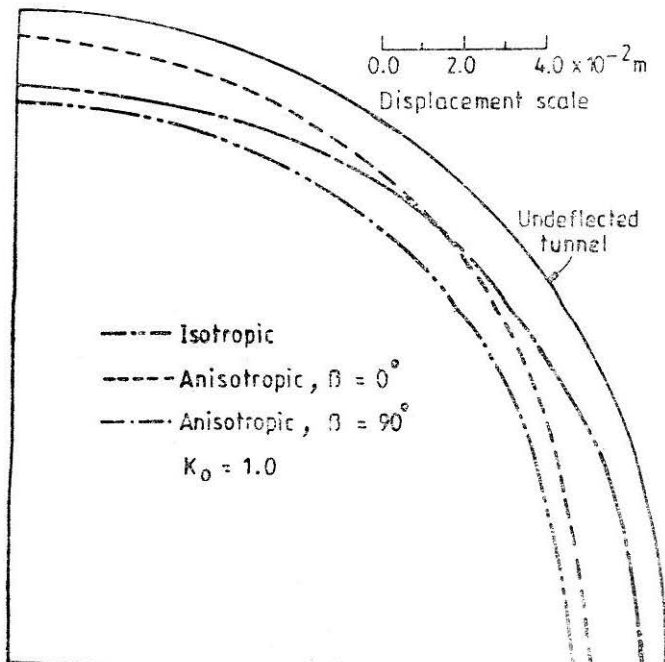
FIGURE 3 Finite Element Mesh for D-type Tunnel

FIGURE 4 Deformed Shape of Circular Opening for $K_o = 0.5$

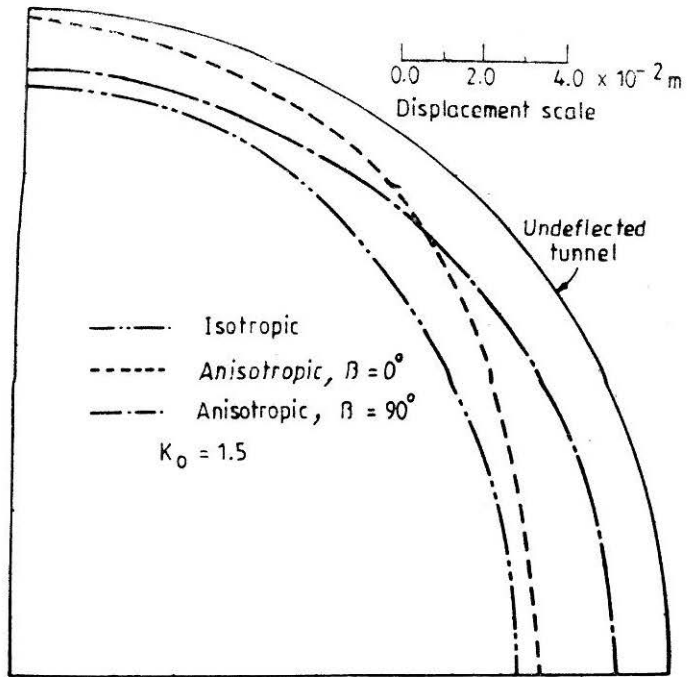**FIGURE 5 Deformed Shape of Circular Opening for $K_o = 1.0$**

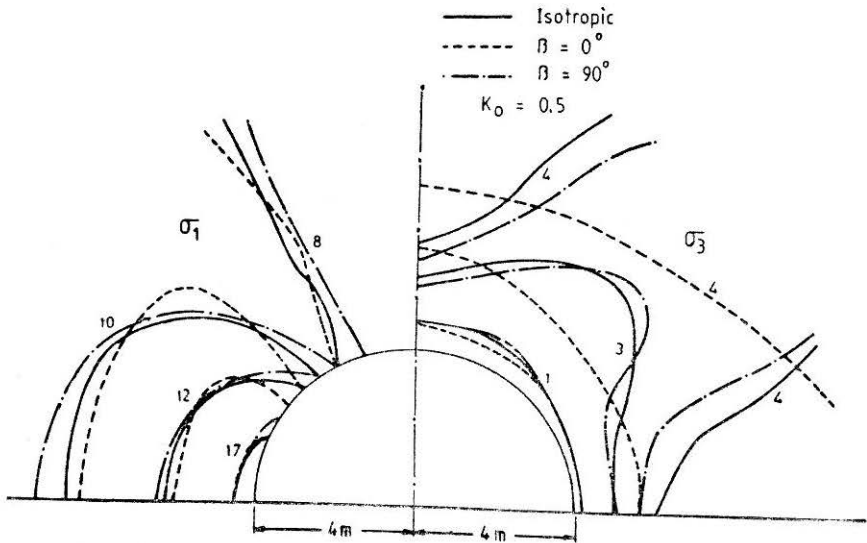**FIGURE 6 Deformed Shape of Circular Opening for $K_o = 1.5$**

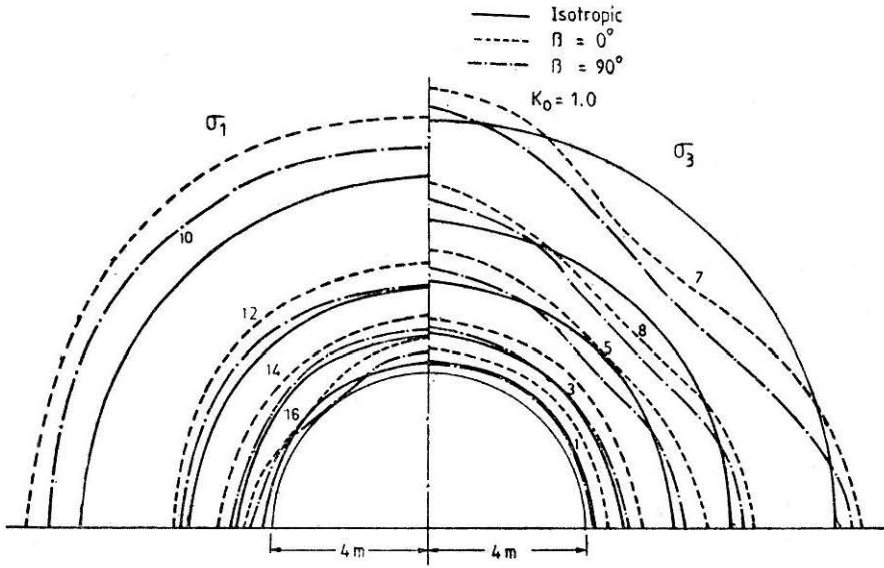**FIGURE 7 Principal Stress Contours for Circular Tunnel, $K_o = 0.5$**

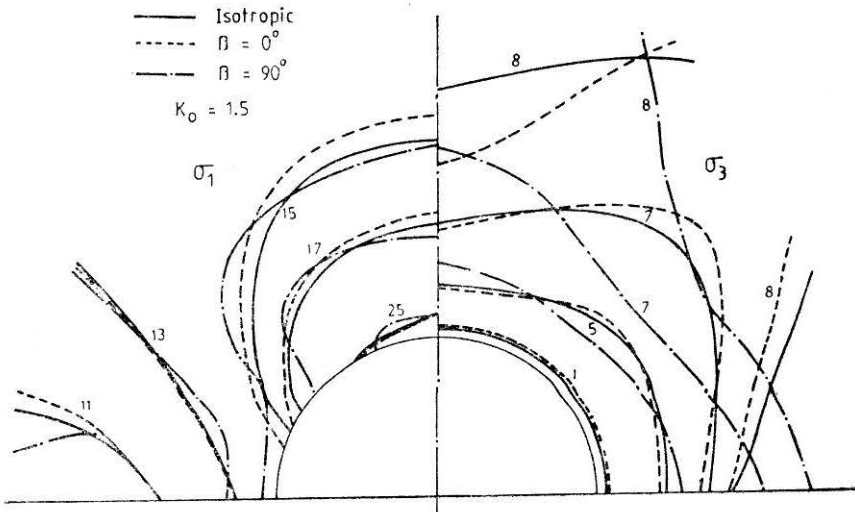FIGURE 8 Principal Stress Contours for Circular Tunnel, $K_o = 1.0$

FIGURE 9 Principal Stress Contours for Circular Tunnel, $K_o = 1.5$

have similar trend whereas the nature of contours for $\beta = 0°$ is different. Near the boundary, the contours for the three cases are close but away from the boundary, they are farther apart. For the same principal stress value, the zone of influence is more for $\beta = 90°$ and least for $\beta = 0°$ and the isotropic case is in between the two cases.

As shown in Fig. 8, for $K_o = 1$, stress contours are concentric, away from the boundary of the tunnel in the case of major principal stresses and near the boundary in the case of minor principal stresses. The zone of influence is greater for $\beta = 0°$ and smaller for isotropic case. The zone for $\beta = 90°$ case falls in between isotropic and $\beta = 0°$ cases.

The contours for $K_o = 1.5$ are plotted in Fig. 9. The major principal stress near the crown is 25.0, which is the highest, of all the three insitu stress ratios considered in the analysis. In case of minor principal stresses, along the crown and springing, the zone of influence is greater for $\beta = 90°$ case, however, at about 45°, $\beta = 0°$ case gives the larger zone of influence. Isotropic and $\beta = 0°$ cases follow similar trend. Major principal stress contours do not follow any trend. Thus it is seen that the variation of principal stresses is affected by both the insitu stress ratio and anisotropy.

D-type Tunnel

(a) *Deformed Shape*: The deformed shape of D-type tunnel is shown in Figs. 10 to 12 for $K_o = 0.5$, 1.0 and 1.5, respectively. The displacements
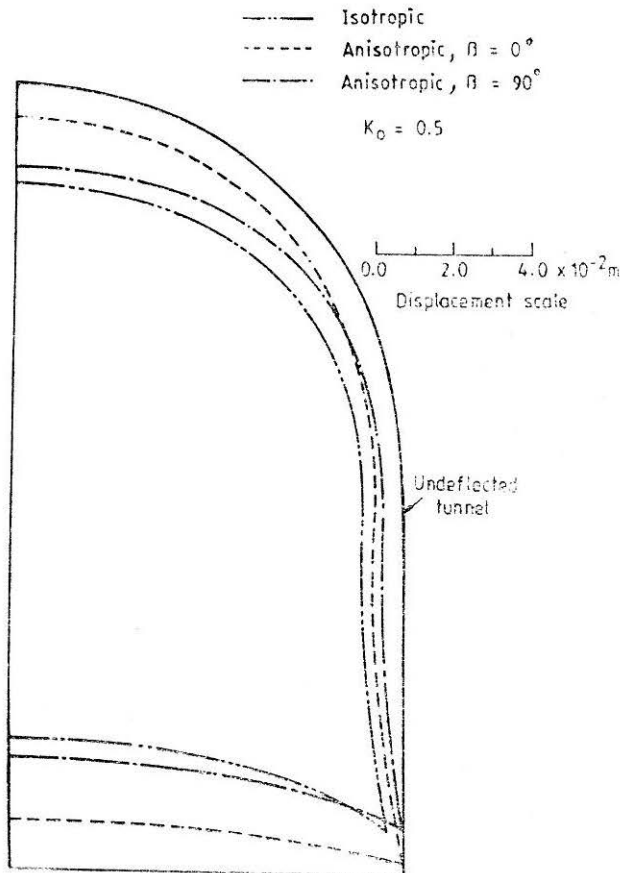

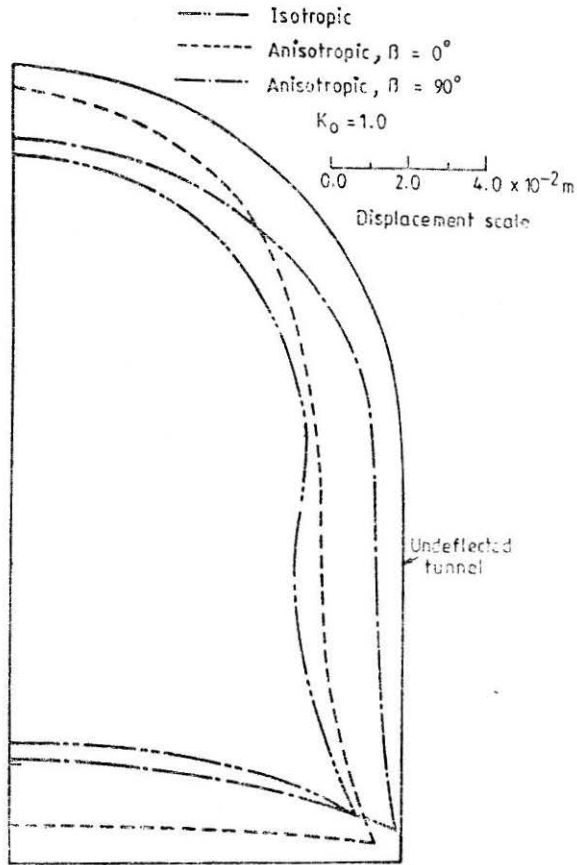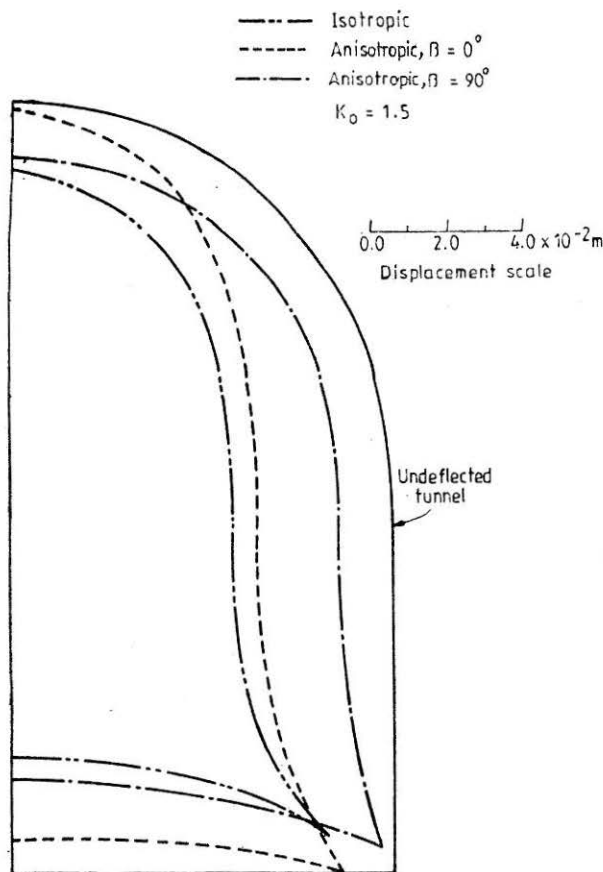FIGURE 10. Deformed Shape of D-type Opening for $K_o = 0.5$

FIGURE 11 Deformed Shape of D-type Opening for $K_o = 1.0$

corresponding to both isotropic and anisotropic cases are plotted in these figures. The displacement at crown reduces with increase in K_o value and at springing, the displacement increases with increase in stress ratio. This behaviour is very similar to that observed for circular tunnel. The reduction in displacement with increase in K_o value is marginal at invert level. The displacements corresponding to anisotropic case are lower than those for isotropic case for all the three stress ratios. The anisotropic case with $\beta = 0°$ gives less displacements at crown and

FIGURE 12 Deformed Shape of D-type Opening for $K_o = 1.5$

invert and larger displacement at springing as compared to $\beta = 90°$. As is seen from these figures, the maximum difference in displacements is for $K_o = 1.5$. Thus anisotropy along with stresss ratio affects the displacements significantly as was observed for circular tunnel.

(b) *Principal Stresses*: It was easy to superpose the principal stress contours for isotropic, $\beta = 0°$ and $\beta = 90°$ cases for each K_o value in case of circular tunnel. For the D-type tunnel, superposition of the contours was attempted but the contours for the three cases were not distinct and the figures did not have the clarity. Therefore, the contours are given for individual cases.

The principal stress contours for $K_o = 0.5$ are plotted in Figs. 13 (a-c) for three cases of isotropy and anisotropy. By comparing the three
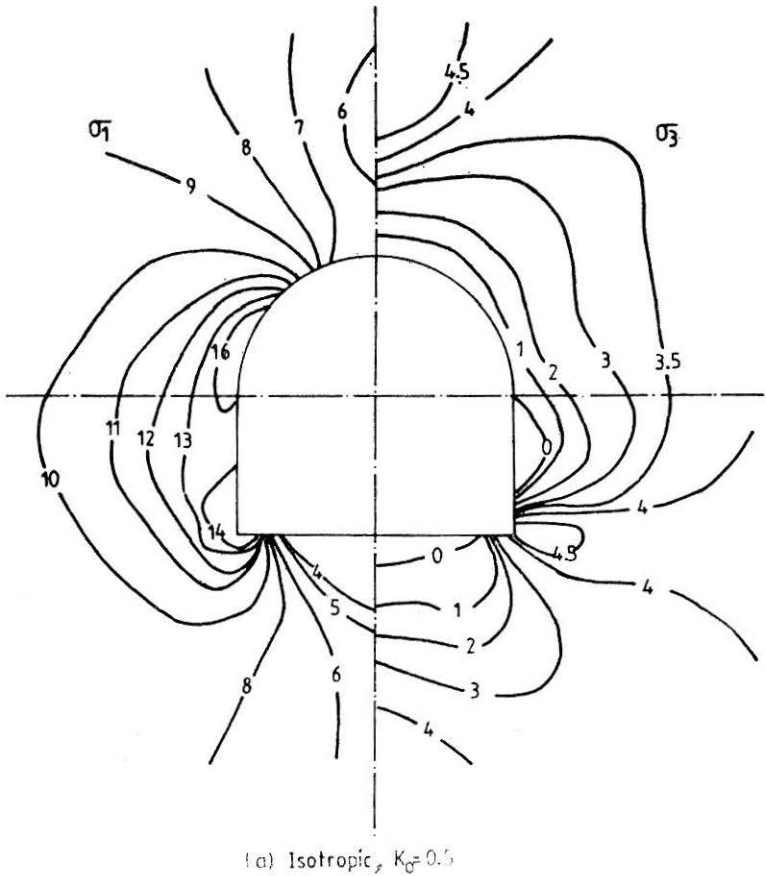
(a) Isotropic, $K_o = 0.5$

FIGURE 13 (a) **Principal Stress Contours for D-type Tunnel, Isotropic, $K_o = 0.5$**

figures, it is seen that the zone of influence extends to a greater distance for $\beta = 90°$ case and is least for $\beta = 0°$ case. Thus, the nature is very similar to that observed in case of the circular tunnel.

Figures 14 (a-c) show the stress contours for $K_o = 1$. For isotropic case, the contours are concentric in the upper circular portion but the degree of concentricity reduces in case of anisotropic rock medium. On the sides and crown, the zone of influence is greater for $\beta = 90°$, and at the bottom, $\beta = 0°$ case gives larger influence zone.

For $K_o = 1.5$, the stress contours are plotted in Figs. 15 (a-c). The major principal stresses near the crown and corner are greater than those for $K_o = 0.5$ and 1.0. In the side and crown portions, zone of influence
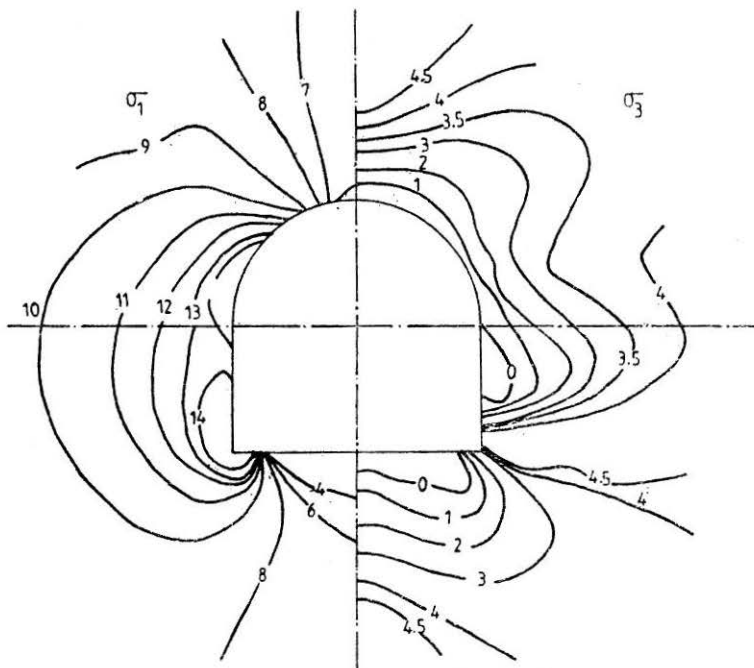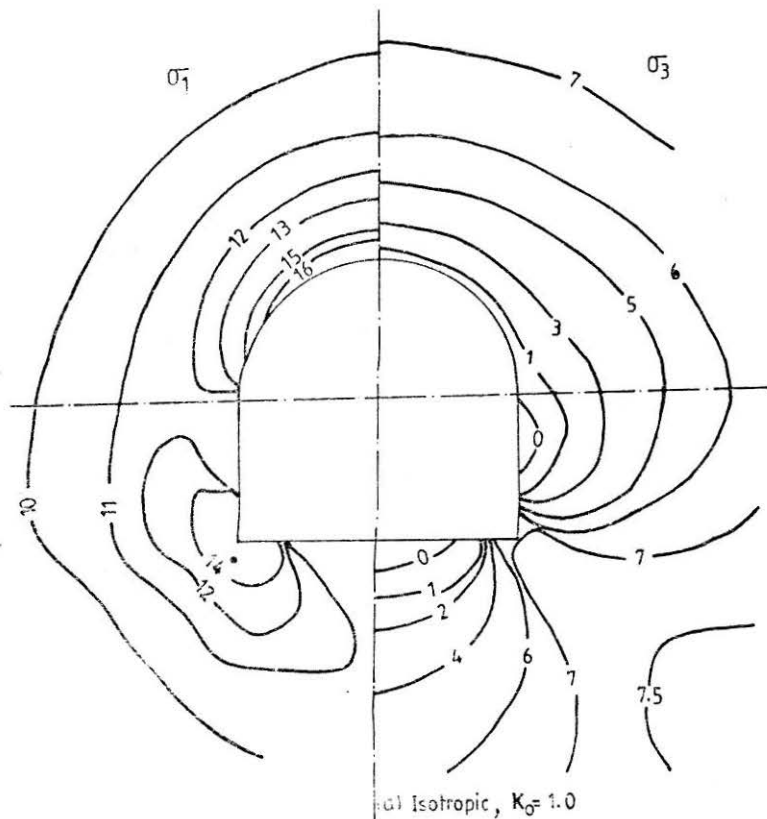
(b) Anisotropic, $\beta = 0°$, $K_0 = 0.5$
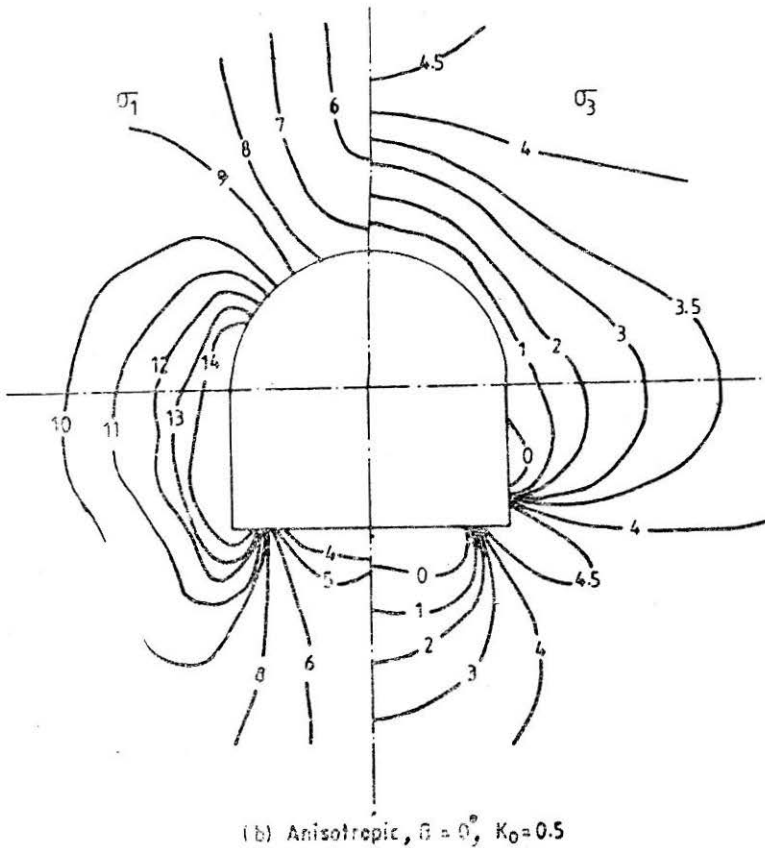
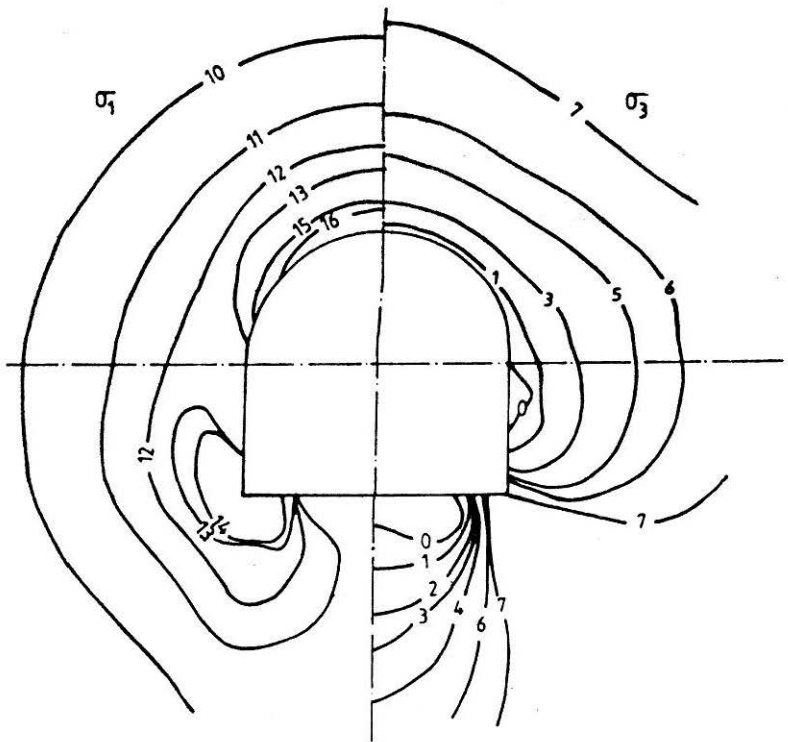**FIGURE 13 (b) Principal Stress Contours for D-type Tunnel, Anisotropic, $\beta = 0°$,**
$K_o = 0.5$

(minor principal stress) is greater for $\beta = 90°$ case, and at bottom and at 45° in circular portion, it is greater for $\beta = 0°$ case. No particular trend is followed by major principal stress contours. It is seen from Figs. 13 to 15 that there are tension zones along side walls and bottom in case of minor principal stress and there is stress concentration at the corner in case of major principal stress. However, the tension zone extends to a very small distance.

The effect of anisotropy on the stress variation is not that much pronounced as is observed on deformation. The insitu stress ratio affects the stresses significantly.

Conclusion

Circular and D-type tunnels have been analysed for three insitu stress ratios ($K_o = 0.5$, 1.0 and 1.5) for three cases, viz. isotropic, anisotropic

(c) Anisotropic, β = 90°, K₀ = 0.5

FIGURE 13 (c) **Principal Stress Contours for D-type Tunnel, Anisotropic, $\beta=90°, K_o=0.5$**

(a) Isotropic, K₀ = 1.0

FIGURE 14 (a) **Principal Stress Contours for D-type Tunnel, Isotropic, $K_o = 1.0$**

(b) Anisotropic, β = 0°, K₀ = 1.0

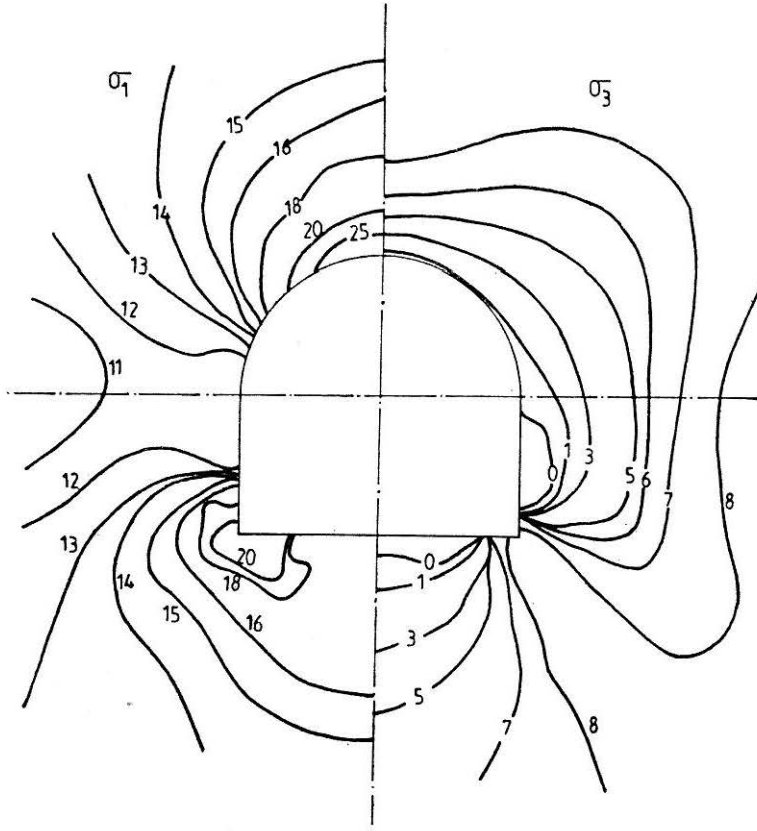**FIGURE 14** (*b*) **Principal Stress Contours for D-type Tunnel, Anisotropic, $\beta = 0°$, $K_o = 1.0$**
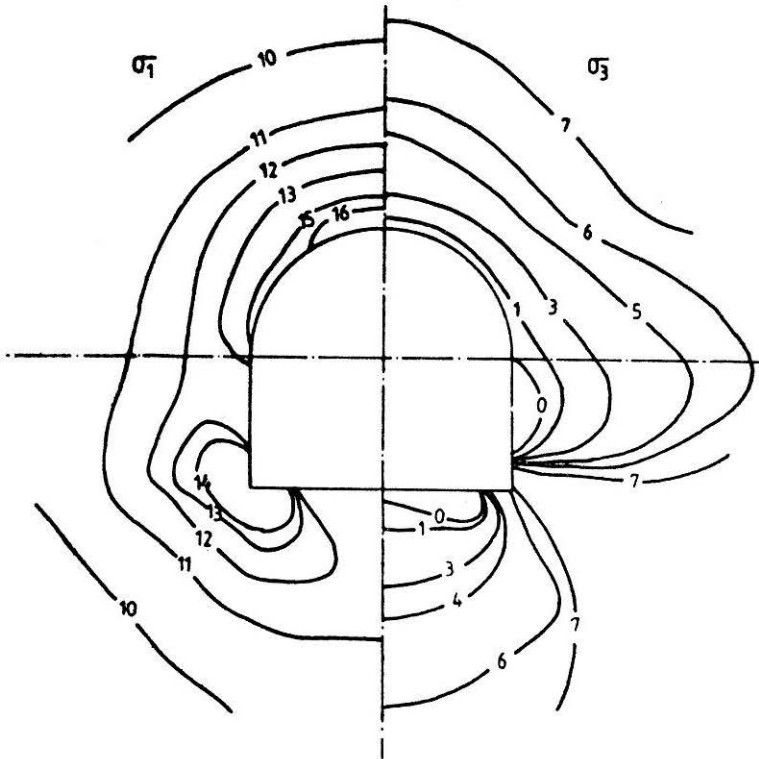

(c) Anisotropic, β = 90°, K₀ = 1.0

FIGURE 14 (*c*) **Principal Stress Contours for D-type Tunnel, Anisotropic, $\beta = 90°$, $K_o = 1.0$**

(a) Isotropic, $K_0 = 1.5$

FIGURE 15 (a) **Principal Stress Contours for D-type Tunnel, Isotropic, $K_o = 1.5$**

with $\beta = 0$ and $90°$. Deformations are smaller for the anisotropic case as compared to isotropic case for all the three stress ratios whether it is circular or D-type tunnel. For both the openings, the anisotropic case with $\beta = 0°$ gives less deformations at crown and invert and larger displacement at the springing as compared to $\beta = 90°$ case. Further, deformations at crown decrease with increase in the stress ratio for all the three cases of isotropy and anisotropy.

In case of circular tunnel for all the three cases, the major principal
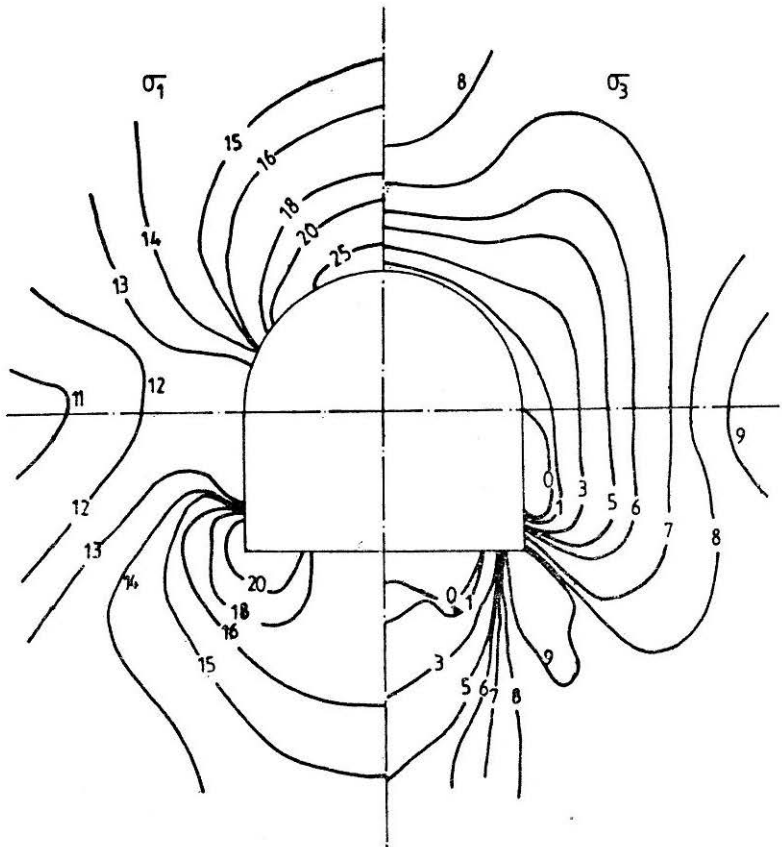
(b)   Anisotropic, $\beta = 0^\circ$, $K_0 = 1.5$

FIGURE 15 (b) Principal Stress Contours for D-type Tunnel, Anisotorpic, $\beta = 0^\circ$, $K_o = 1.5$

stress is higher near the springing for $K_o = 0.5$ and near the crown for $K_o = 1.5$. For D-type opening, the stress concentration is at the corner for all the stress ratios. In addition, the major principal stress is higher near the springing and side walls for $K_o = 0.5$ and near the crown for $K_o = 1.5$. The zone of influence of principal stresses is affected by the anisotropy for all the three stress ratios. But the effect is not that significant as in case of deformations. The above conclusions are based on the rock properties used for the present analysis.
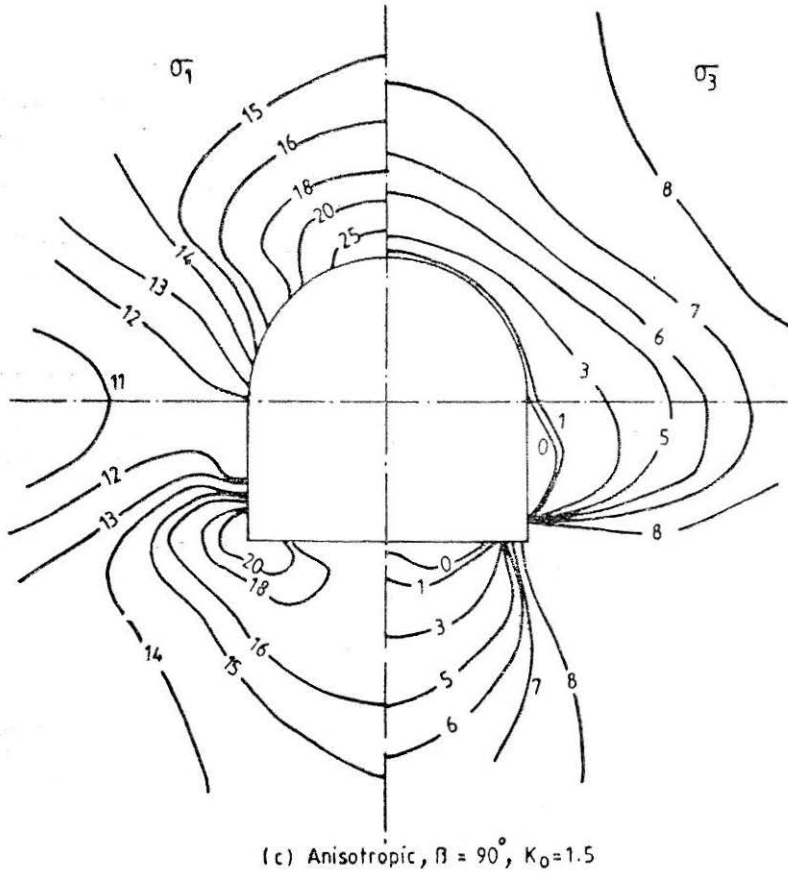
(c) Anisotropic, $\beta = 90°$, $K_0 = 1.5$

FIGURE 15 (*c*) **Principal Stress Contours for D-type Tunnel, Anisotropic, $\beta = 90°$, $K_0 = 1.5$**

References

LAMA, R.D. and VUTUKURI, V.S. (1978): *"Handbook on Mechanical Properties of Rocks"*, Trans. Tech. Publications, Clausthal, Vol. 2.

BARLA, G. (1974): "Rock Anisotropy-Theory and Laboratory Testing", In *'Rock Mechanics'*. Edited by L. Muller, University of Karlsucke. Udine.

OBERT, L. and DUVALL, W.I. (1967): *"Rock Mechanics and the Design of Structures in Rock"*. John Wiley & Sons, New York.

ZIENKIEWICZ, O.C. (1977); *"The Finite Element Method"*, McGraw-Hill Book Company, London.

SHARMA, M.K. (1984) ; *"Analysis of Tunnels by Finite Element Method,"* unpublished M. Tech. Thesis, Department of Civil Engineering I.I.T. Delhi.